Measurements of Frictional Heating in Granite

DAVID A. LOCKNER AND PAUL G. OKUBO

U.S. Geological Survey, Menlo Park, California 94025

A large (150 × 150 × 40 cm) granite sample, sawn diagonally in half to simulate a fault, was deformed in a biaxial rock press at normal stress up to 6.41 MPa. Displacements and local shear stress were monitored along the fault (200 × 40 cm). Temperature transients as large as 10 m°C were recorded following stick slip events at distances of 0.2 to 1.0 cm from the fault and were related to stress, displacement, and total work. The temperature measurements were used to calculate the heat generated on the fault during slip. Frictional heating was found to be 94 ± 2% of the total work expended in each event, implying a seismic efficiency of 4-8 %. When water was injected onto the fault, both fractional stress drop and static frictional stress increased. The efficiency of frictional heating was not lowered by the presence of water. Heat generated during deformation of a 0.15-cm-thick layer of simulated gouge was also measured for sliding rates from 0.09 to 9.1 μm/s. In these gouge experiments, temperature rises were less than 0.1°C and were proportional to sliding rate.

INTRODUCTION

Many people have suggested that frictional heating could play an important role in earthquake dynamics. *Jaeger* [1942], *McKenzie and Brune* [1972], and *Richards* [1976] suggested that frictional heating during earthquakes could lead to melting on the fault surface and subsequently to a decrease in shear strength. McKenzie and Brune cite the occurrence of mylonites in fault zones as possibly representing recrystallized gouge material. *Sibson et al.* [1979] found numerous occurrences of pseudotachylytes in the Alpine fault zone which they suggest were the result of frictional heating.

If water is present along faulting surfaces, the dynamics can become much more complicated. *Sibson* [1973] showed how constant-volume heating of water in the fault zone could lead to essentially zero shear strength. This could occur if the permeability of the fault zone is very low. *Raleigh* [1977] suggested that frictional heating could dehydrate fault gouge material, liberating a sufficient quantity of water to reduce friction. *Lachenbruch* [1980] analyzed the interaction of a number of parameters involved in the dynamics of a wet fault and showed that under the proper conditions, thermal expansion of pore fluids due to frictional heating could lead to a partial or total drop in shear strength or, conversely, dilatation in and around the fault zone could lead to increased shear strength. He also concluded that if permeability exceeds approximately 100 mdarcies, all of these thermomechanical effects can probably be ignored. Thus depending on the relative importance of a number of processes, dynamic friction could vary considerably during earthquakes.

The absence of a localized heat flow anomaly along the San Andreas fault system provides important data from which to infer the driving stresses along the plate boundaries in California [*Brune et al.*, 1969; *Lachenbruch and Sass*, 1980]. However, relating heat flow to regional tectonics depends on a number of poorly known processes, including seismic versus frictional heating efficiency and the flow of groundwater.

Few laboratory data exist for the frictional heating of crystalline rocks. Surface heating of laboratory samples has been measured with thermal dyes by *Teufel and Logan* [1978]. With this technique, they reported temperature rises in excess of 1000°C, presumably at asperity contacts, for laboratory samples failing in 'stick slip.' However, it is not entirely clear [*Byerlee*, 1977] how

these thermal dyes respond to stress, as in these experiments, and consequently, they may not give an accurate indication of temperature for these conditions.

It should be emphasized that rapid changes in friction during earthquakes resulting from sudden pore pressure or temperature transients have never been observed. Our understanding of these processes is still on a theoretical level. We therefore conducted a series of experiments measuring the heat generated during sliding on a simulated fault in granite in order to test some of the basic hypotheses of frictional heating of faults. These hypotheses include the following: (1) most of the energy released during stick slip goes into heating the fault and (2) the presence of water will reduce dynamic friction by lubricating the fault. We first studied how frictional heating was related to total energy expended during stick slip and then how heating of the fault was affected by the presence of water and simulated fault gouge. After parameterizing these variables for large-scale laboratory experiments, we study the implications that these results have for theories of frictional heating and energy budgeting for earthquakes.

EXPERIMENTAL METHOD

All experiments were performed on a 150 × 150 × 40 cm sample of Sierra gray granite from Raymond, California, sawn in two along the diagonal to simulate a fault. The sample was deformed in a large-scale biaxial press shown in Figure 1. The design load capacity of the press is 2.2×10^7 N and 1.2×10^7 N for the major and minor loading axes, respectively. Hydraulic flatjacks, wedged between the loading frame and the sample, are used to load the sample independently along the two axes [*Dieterich*, 1981]. High-speed hydraulic valves under computer control are used to adjust the load to an accuracy of 0.01 MPa. The sliding surfaces of the sample are 200 × 40 cm and are oriented at 45° to the major axes. To assure good mating of the sliding surfaces, the sample halves were lapped together with 240 grit abrasive to a profilometer measured surface roughness of 0.5 μm. To inject water onto the simulated fault surface, 12 holes 1.27 cm in diameter were drilled parallel to the fault, 3.81 cm from the fault surface (Figure 2). 0.238-cm-diameter holes were then drilled from the fault to intersect the main feeder holes [*Lockner et al.*, 1982]. Finally, 0.05-cm-deep channels were scribed on the fault surface to assure good communication of the pore fluid with the fault.

Temperatures were measured at three locations (Figure 2) with thermistors, encased in glass beads and vinyl dipped for hermetic sealing. The overall diameter of the thermistors is 0.15 cm. The
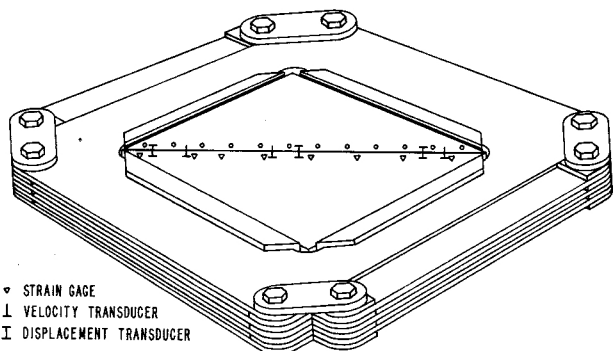
Fig. 1. Schematic diagram of granite sample mounted in loading frame. Locations of strain gages, velocity transducers, displacement transducers, and injection ports are shown.

thermistors were cemented in boreholes at depths of 0.2, 0.5, and 1.0 cm from the fault surface. Granite caps were then cemented over the tops of the thermistors and ground flush with the sliding surface. Each thermistor was used as a leg in an op amp amplifier circuit. The output of each circuit was recorded on strip chart and also on digitized computer files, giving a sensitivity of 0.1 m°C and a response time of about 0.1 s.

Eight pairs of semiconductor strain gages were mounted along the top of the fault surface to monitor the local shear strains (Figure 2). By assuming pure elastic deformation of the sample, these strains were used to infer local shear stresses along the fault [Okubo and Dieterich, 1981]. Three high-speed velocity transducers and one DCDT displacement transducer were also mounted along the fault.

Two sets of data were recorded and stored for each experiment. First, slow-speed records, sampled once every second on a 12-bit analog-to-digital converter, were taken of flatjack pressures, strain gage, DCDT, and temperature outputs. Second, a 10-channel, 10-bit digital storage module recorded strain gage and velocity transducer outputs during each stick slip event. These high-speed records store 4096 samples per channel at sampling intervals as short as 5 μs. After each event, the contents of these high-speed buffers were transferred to permanent disk storage.

A number of experiments were conducted to measure the heat generated during sliding at normal stresses ranging from 0.69 to 6.41 MPa. These experiments fall into three main groups: (1) slip on dry fault with no gouge, (2) slip on wet fault with no gouge, and (3) slip on dry fault with gouge. In the experiments without gouge, shear and normal stress were controlled. In the gouge experiments, a 0.15-cm-thick layer of sorted Ottawa sand (nominal grain size of 0.025 cm) was placed between the sample halves.

A series of creep experiments was performed at constant shear and normal stress. This was followed by a series of experiments at constant sliding rates varying from 0.09 to 9.1 μm/s. Shear (τ) and normal (σ_n) stresses are given by $\tau = (\sigma_1 - \sigma_2)/2$ and $\sigma_n = (\sigma_1 + \sigma_2)/2$, where σ_1 and σ_2 are the pressures in the major and minor axis directions, respectively. In the gouge experiments, while the sliding rate was controlled, σ_2 was held constant. As a result, both shear and normal stress varied as σ_1 varied in these experiments.

In the wet experiments, filtered tap water was injected onto the fault at constant pressure in the range 0-3.45 MPa. Because the fault was left unsealed, close mating of the fault surfaces was required to maintain pore pressure. Injection pressures of approximately 1.5 times the applied normal stress could be maintained without significant leakage of pore fluid. Because the fault surface was unsealed, a pore pressure gradient must exist in the 5-cm border between the pore pressure channels and the open air (Figure 2) over which the pore pressure dropped to 1 atm. This means that as much as 25% of the fault surface could have less than the prescribed injection pressure, explaining why we were able to overpressure the fault zone. This experimental design complicates the analysis of the injection experiments but nevertheless was used due to its simplicity.

The temperature of the fault was not measured directly for two reasons. A sensor placed directly in the fault zone would most likely be destroyed during a violent stick slip event. Also, stick slip events last for 2 to 4 ms, so a probe capable of measuring the resulting temperature transients would need a response time of the order of 1 ms. We therefore decided to determine the heat generated on the fault indirectly by placing thermistors 0.2-1.0 cm from the fault (thermistors used were 0.15 cm in diameter). We assume that during a stick slip event, heat is generated uniformly over the entire fault surface and that consequently the propagation of temperature transients away from the fault can be accurately represented by a simple one-dimensional heat flow model. In this case, temperature transients 0.2 to 1.0 cm from the fault can be expected to peak on the order of seconds rather than milliseconds after the rupture. By comparing temperature transients recorded at various distances from the fault to corresponding temperature curves computed from an analytic solution to the one-dimensional heat flow model, the total heat generated during stick slip events is inferred. In addition, since the stress-displacement history for
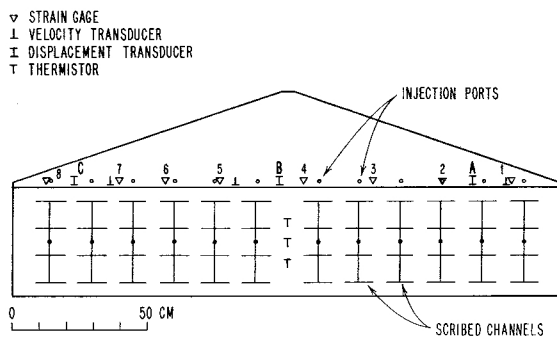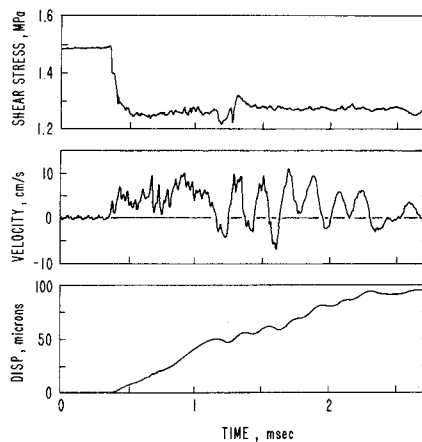

Fig. 2. View of granite sample half showing sensor locations and scribed channels used to distribute pore fluid on fault surface. Strain gages, actually mounted on other sample half, are included here to give relative locations.

Fig. 3. High-speed local shear stress and sliding velocity records at station 5 for stick slip event at $\sigma_n = 2.76$ MPa. 0.2 ms period oscillations are ringing of transducer. Displacement is obtained by integrating velocity curve.

each event is recorded on the high-speed records, the total heat generated can be compared to the work performed during sliding.

RESULTS

Dry Experiments

The first series of experiments was performed on dry sliding surfaces without gouge. In each experiment, normal stress was held constant (ranging from 0 to 4.41 MPa), while shear stress was increased at a constant rate (in the range 3.4×10^{-3} to 2.8×10^{-2} MPa/s). This continued until failure, at which point the computer automatically held the shear stress at its residual level. The temperature transient was then recorded for a period of 200-1000 s.

The first step in the analysis is to relate these temperature transients to the total work done during sliding. To determine the work done, we use the high-speed stress and sliding velocity records shown in Figure 3. The velocity record is integrated once in time to obtain displacement. The longer-period oscillations beginning about 1 ms after the start of the event represent fundamental modes of the press and a resonant mode in the velocity transducers excited by the stick slip event. Figure 3 shows that after the stick slip event begins with a rapid drop in shear stress of 0.22 MPa to the dynamic friction level, sliding lasts for approximately 2 ms, while shear stress remains at a nearly constant level. Plotting shear stress as a function of displacement (Figure 4), we observe slip-weakening behavior on the fault similar to that discussed by *Okubo and Dieterich* [1981], *Andrews* [1976], and *Ida* [1972]. The diagonal straight line in Figure 4 starting at τ_i represents the unloading curve of the rock press. This unloading curve of 33 MPa/cm was determined by measuring the static stress before and after a series of stick slip events to determine the stiffness of the loading frame and sample and is independent of normal stress over the range used in these experiments. The area under the unloading curve is the total energy released during the stick slip event and will now be compared to the temperature data.
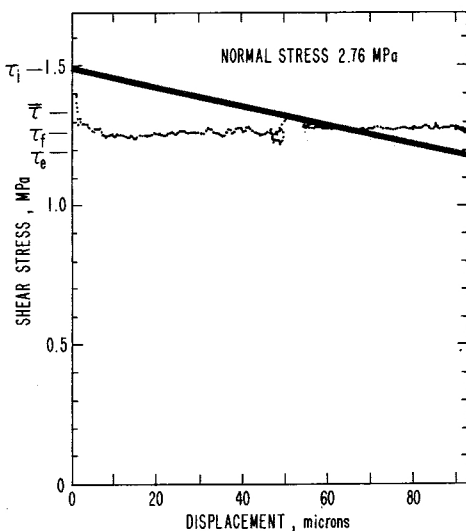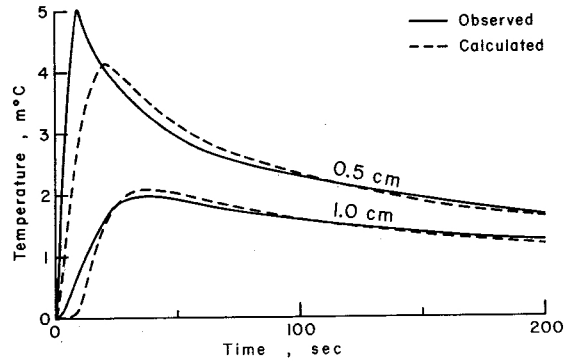

Fig. 5. Temperature plots (solid curves) for two thermistors following stick slip event 12. Dashed curves are corresponding solutions to one-dimensional heat flow model.

Figure 5 shows temperature transients and corresponding analytic solutions 0.5 and 1.0 cm from the fault surface for stick slip event #12. The analytic solutions (see discussion below) are scaled to agree with the observed temperatures 100 s after the event. Both observed temperatures rise faster than the corresponding analytic solutions but then are in good agreement after about 40 s. We attribute this early temperature rise to heat generated locally about the thermistors in response to the sudden strains accompanying stick slip. These local effects should dissipate much faster than the temperature transients produced over the entire fault surface during frictional sliding. For this reason, in the following calculations we use temperature readings 100 s after stick slip to allow sufficient time for the local transient effects to decay. These temperature rises are plotted as a function of total work in Figure 6. The good linear fit shows that the temperature rise is proportional to total work done. Similar comparisons of temperature to normal stress, shear stress, shear stress drop, and displacement show that temperature is not linearly related to any of these parameters over the range studied.

The temperature transients recorded for the 0.2 cm thermistor were consistently lower than expected from the analytic solution. In addition, the strong temperature transient that should occur within 1 s following stick slip was greatly attenuated at this station and was less than the transient measured at the 0.5 cm station. A surface profile conducted after the experiments revealed that the rock was pitted at this thermistor location. Because of the

Fig. 4. Local stress-displacement curve for event in Figure 3. Diagonal line of slope 33 MPa/cm, beginning at initial stress, τ_i, is unloading curve of press. Area under this curve is total work expended, $W_T = 0.5(\tau_i + \tau_e)u = \bar{\tau}u$; τ_f is average dynamic shear strength; $\tau_f u$ represents work expended in frictional heating of fault.
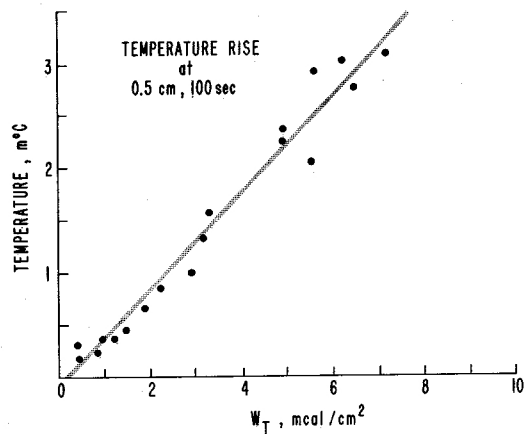

Fig. 6. Plot of temperature rise 0.5 cm from fault and 100 s after stick slip versus total work W_T for all dry events. Line is least squares fit to data.
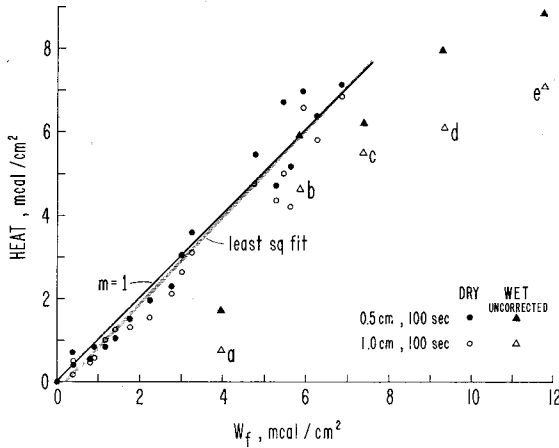
Fig. 7. Plot of heat generated during stick slip versus frictional sliding energy (obtained from stress-displacement curves) for wet and dry events. Least squares fit (stippled line) to dry events has slope 0.96 ± 0.06. Wet events are uncorrected for effect of water in fault zone (see text). Pore pressures for wet events are $a = 2.76$, $b = 1.31$, $c = d = 0.34$, $e = 0$ MPa.

surface irregularities, less than half of the surface directly over the thermistor was in contact during sliding, resulting in a local cool spot. This interpretation is further confirmed by the fact that when gouge was placed between the sliding surfaces, the 0.2 cm thermistor responded in a manner consistent with the other thermistor. We therefore do not use the 0.2 cm temperature transients to interpret the stick slip data.

We next determine the actual amount of work that goes into heating the fault. To calculate the heat generated, temperatures measured 100 s after slip are compared to temperatures calculated from an analytic solution to a one-dimensional heat conduction model, satisfying

$$\frac{\partial^2 T}{\partial x^2} - \frac{1}{\alpha} \frac{\partial T}{\partial t} = 0 \qquad (1)$$

The solution for an instantaneous plane source at $x = 0$ and time $t = 0$ is

$$T(x,t) = t^{-1/2} \exp \left[-\left(\frac{x}{a_\tau} \right)^2 \right] \qquad (2)$$

where $a_\tau = \sqrt{4\alpha t}$ is the conduction half width. This represents the release of the quantity of heat per unit area $2k(\pi/\alpha)^{1/2}$ [Carslaw and Jaeger, 1959]. Since the duration of sliding is so short compared to the times over which temperatures are measured, the analytic solution (2) is a good approximation.

The frictional work per unit area W_f can be computed in two ways. First, it is the work expended on the fault during sliding

$$W_f = \tau_f u \qquad (3)$$

where τ_f is the shear stress on the fault during sliding and u is displacement. Frictional work can also be related to the heat per unit area generated during slip:

$$H_f = \sqrt{\pi} \ \frac{k}{\alpha} \ a_\tau \ T_{(x,t)} \ \exp \left[+\left(\frac{x}{a_\tau} \right)^2 \right] \qquad (4)$$

Since both $T(x, t)$ and $\tau_f u$ are measured, we can test the validity of equating W_f and H_f. Nominal values used in the analytic solution are $\alpha = 0.013$ cm^2/s and $k = 0.007$ cal/°C cm s [Lachenbruch, 1968]. The sliding surfaces of the sample are smooth and deformed at relatively low stress, so that little new surface area is created during stick slip events [Engelder, 1978]. In this case, we expect that the area beneath the sliding friction curve τ_f in Figure 4 represents the frictional work (equation (3)). Frictional heating, computed by (4), is plotted as a function of frictional sliding energy in Figure 7. This is done for temperatures both 0.5 and 1.0 cm from the fault. Temperatures are picked, as described earlier, 100 s after rupture. If the heat generated is identical to the sliding friction energy, we would expect the data to fall on a line of slope 1. The least squares fit to the combined data is drawn in Figure 7 and has a slope of 1.04. A t test analysis of this data gives, at the 95% confidence level, an uncertainty of ±0.06. Figure 7 shows a small systematic difference between the 0.5 and 1.0 cm data. Fits to these two subsets yield slopes of 1.09 ± 0.09 and 0.98 ± 0.07 for the 0.5 and 1.0 cm thermistors, respectively. A possible cause of the difference in slopes is local variations in normal stress at the thermistor sites. In this case, the best estimate is obtained by combining all the measurements. We conclude that to within the precision of the data, the simple frictional sliding model adequately describes our observations.

We can now compare the frictional heating to the total work expended during stick slip $W_T = \bar{\tau} u$ where $\bar{\tau} = (\tau_i + \tau_e)/2$ (Figure 4). The result is that 88 ± 6% of the total energy released is converted to heat on the fault. Much of the 6% uncertainty in the frictional heating estimates result of the compounding of errors in (4) when computing heat from temperature. Because (3) and (4) can be equated, measurements of frictional work expended during stick slip can be computed from (3). When calculated in this manner, frictional heating accounts for 94 ± 2% of the total work. This estimate is based only on measurements of shear stress and displacement and not on temperature. Since the amount of new surface area created in these low stress experiments due to comminution of the sliding surfaces is negligible, the remaining work must go into radiated seismic energy. Therefore the seismic efficiency for these experiments is between 4 and 8%. A summary of slip parameters for all events is given in Table 1.

Water Injection

A series of experiments were performed at constant normal stress of 3.45 MPa with water injected onto the fault at different pressures. Water injection pressures were held constant during each run with values of 0.0, 0.34, 1.31, and 2.76 MPa. Heat was calculated from the temperature transients in the same way as for the dry experiments. As seen in Figure 7, it appears that the heat generated accounts for only about 80% of the work expended in sliding.

We now examine how the presence of water in the system will affect the accuracy of these measurements. If all of the frictional sliding energy is in fact converted to heat, then the resulting decrease in the observed temperature transients would require a two-fold increase in heat conductivity. This is too large a change to be brought about by the small amount of water that can be contained in the pores. In addition, because of the low porosity of the granite, the specific heat of water-saturated Sierra granite is only a few percent larger than dry Sierra granite. The observed temperature deficits cannot be explained by this small change in specific heat.

TABLE 1. Summary of Slip Parameters

Event	Pore Press, MPa	Normal Stress, MPa	τ_i, MPa	$\bar{\tau}$, MPa	τ_f, MPa	u, μm	T(100 s), m°C		Hf, mcal/cm²		Wf, mcal/cm²	WT, mcal/cm²	Wf/WT
							0.5 cm	1.0 cm	0.5 cm	1.0cm			
1	dry	0.55	0.40	0.32	0.34	48	0.3	0.1	0.7	0.2	0.39	0.37	1.05
2	dry	0.55	0.41	0.33	0.35	50	0.2	0.2	0.5	0.5	0.42	0.39	1.08
3	dry	1.10	0.68	0.58	0.57	60	0.2	0.2	0.6	0.5	0.82	0.83	0.99
4	dry	1.10	0.70	0.59	0.59	64	0.4	0.2	0.8	0.6	0.90	0.90	1.00
5	dry	1.66	0.94	0.84	0.80	62	0.4	0.4	0.8	1.0	1.18	1.24	0.95
6	dry	1.66	0.98	0.86	0.85	70	0.5	0.5	1.1	1.2	1.42	1.44	0.99
7	dry	2.21	1.21	1.09	1.03	73	0.7	0.5	1.5	1.3	1.80	1.90	0.95
8	dry	2.21	1.26	1.12	1.07	84	0.9	0.6	2.0	1.6	2.15	2.25	0.96
9	dry	2.76	1.49	1.34	1.26	93	1.0	0.8	2.3	2.1	2.80	2.98	0.94
10	dry	2.76	1.53	1.37	1.30	97	1.3	1.0	3.1	2.6	3.01	3.17	0.95
11	dry	3.31	1.83	1.59	1.52	145	2.1	1.6	4.7	4.3	5.27	5.51	0.96
12	dry	3.31	1.83	1.62	1.52	128	2.3	1.6	5.1	4.2	4.65	4.95	0.94
13	dry	4.41	2.34	2.13	1.96	127	3.1	2.4	6.9	6.5	5.95	6.46	0.92
14	dry	4.41	2.40	2.17	2.02	142	3.1	2.5	7.1	6.8	6.85	7.36	0.93
15	dry	4.41	2.21	2.02	1.93	119	2.9	1.9	6.7	5.0	5.49	5.74	0.96
16	dry	4.41	2.27	2.05	1.96	134	2.8	2.2	6.4	5.8	6.27	6.56	0.96
17	dry	4.41	2.07	1.95	1.84	74	1.6	1.2	3.6	3.1	3.25	3.45	0.94
18	dry	4.41	2.20	2.03	1.91	105	2.4	1.8	5.4	4.7	4.99	5.09	0.98
19	dry	3.45	1.98	1.77	1.70	126	-	-	-	-	5.12	5.33	0.96
20	0 (wet)	3.45	2.36	1.93	1.87	262	4.0	2.7	9.0*	7.1*	11.70	12.08	0.97
21	0.34	3.45	2.14	1.84	1.70	182	2.8	2.1	6.2*	5.5*	7.39	8.00	0.92
22	0.34	3.45	2.21	1.85	1.79	218	3.6	2.3	8.0*	6.1*	9.32	9.63	0.97
23	1.31	3.45	1.91	1.66	1.59**	154	2.7	1.8	6.0*	4.7*	5.85**	6.11	0.96**
24	2.76	3.45	1.21	0.95	1.05**	158	0.8	0.3	1.7*	0.8*	3.96**	3.59	1.10**

*Heat estimates are not corrected for presence of water (see text).
**τ_f was measured at the surfce where $P_p = 0$. Therefore these values are upper bounds.

If we consider the fault surface itself, however, and assume that the source of heating during slip is occurring in some narrow zone of deformation of width δ, we can estimate the effect of saturating this zone with water. Assume that a volume fraction, φ, of this zone can be wetted. We let r represent the ratio of the temperature rise at some distance from the fault for a wet experiment to the temperature rise at the same distance for an equivalent dry experiment. This ratio will be nearly constant for all distances. The temperature rise in the heating zone of the dry experiment is given by

$$H = \rho_d \delta c_d T_d \qquad (5)$$

where d denotes values for dry rock, H is heat per unit area, and c is specific heat. For a wet experiment of equivalent heat generation, the heat absorbed by the matrix is simply $\rho_d \delta c_d r T_d$ or rH. The heat absorbed by the water is then

$$(1-r)H = \rho_w \phi \delta c_w r T_d \qquad (6)$$

where w denotes values for water. Rearranging and substituting (5) gives

$$\phi = \frac{1-r}{r} \frac{\rho_d}{\rho_w} \frac{c_d}{c_w} \qquad (7)$$

Using $r = 0.8$, $\rho_d = 2.7$ g/cm³, and $c_d = 0.18$ cal/g°C gives a porosity for the fault zone of 0.13. This is a reasonable value and indicates that the apparent discrepancy in the temperature transients can be accounted for by saturation of the zone of deformation. If the width of the deformation zone is of the order of the fault surface roughness (approximately 1 μm), the seepage of water out of the fault should be small, even for this relatively large porosity. This, in fact, was the case in these experiments.

The presence of water on the sliding surfaces has an interesting effect on the failure process. Premonitory creep is observed for many of the wet stick slip events. This slip generally occurs in the center while one or both ends of the sample remain locked until the stick slip event. Figure 8 shows premonitory creep of the center of the sample for wet surfaces but at zero injection pressure when the sample was loaded at a constant rate. Notice that the creep accelerates, beginning approximately 3 s before the event. Premonitory creep of up to 10 μm is observed for the wet experiments. The amount of creep is not related to the injection pressure. We find that for dry experiments performed on the same finely ground sample, there is no measurable premonitory creep, even for very slow loading rates.

The presence of water on the fault also affects the relative static stress drop $(\tau_i - \tau_e)/\tau_i$ of unstable events. In Figure 9, initial shear stress is plotted as a function of total slip for all events. The stiffness of the loading frame, measured to be 0.33 MPa/cm, can
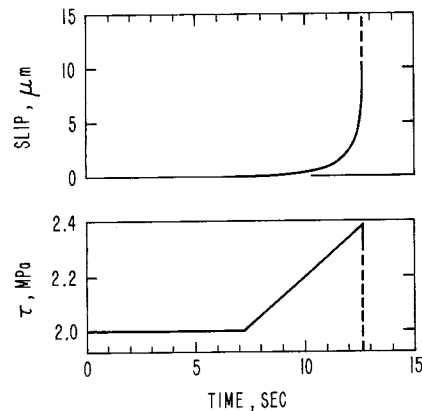

Fig. 8. Premonitory creep for wet fault, zero pore pressure, $\sigma_n = 3.45$ MPa and constant loading rate. No premonitory creep was observed for dry experiments.
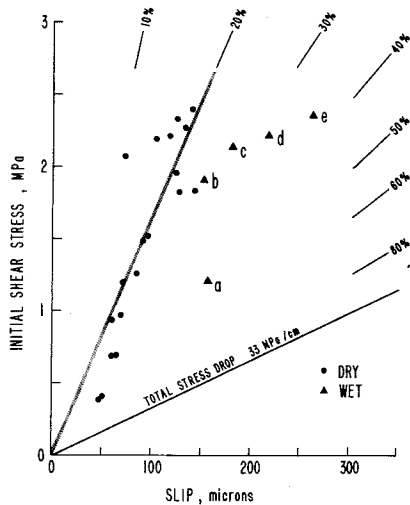
Fig. 9. Plot of initial shear stress versus total slip for wet (triangles) and dry (dots) events. Total stress drops plot along line having slope 33 MPa/cm = machine stiffness. Dry events have relative static shear stress drops of 20%. Effect of water is to increase stress drop. Pore pressures for wet events are $a = 2.76$, $b = 1.31$, $c = d = 0.34$, $e = 0$ MPa.

be used to determine the stress drop of each event from the total displacement. Thus events for which initial stress plots along the line of slope 0_y33_s MPa/cm in Figure 9 would have total stress drops. Dry experiments have static stress drops of about 20% of initial shear stress (or 10% of normal stress). The stress drops for wet experiments are all larger than this, being as high as 40%. If pore pressure rises during slip due to heating of the fault or a sudden reduction in pore volume, τ_f should drop during each event. This does not happen. In Figure 10, both initial and frictional shear stress are plotted as a function of effective pressure. The larger static stress drops for wet events are a result of increased initial stress rather than decreased friction, as discussed by *Lachenbruch* [1980]. Given the small temperature rises measured in these experiments, the lack of variation in dynamic friction actually agrees with Lachenbruch's analysis. This effect is also seen as an increase in the static coefficient of friction μ. For the dry fault, μ is nominally 0.55 but increases to 0.69 for the wet experiment at zero pore pressure. This strengthening effect has been noted by others [*Byerlee*, 1967; *Bowden and Tabor*, 1958] for

highly polished surfaces at low normal stresses and may be related to surface tension effects. This increase in friction apparently reverses at higher normal stress where the presence of water tends to reduce strength.

Gouge Experiments

Two series of experiments were performed with a 0.15-cm-thick layer of Ottawa sand between the sliding surfaces. In the first series, normal stress was held constant at 0.69 MPa, and shear stress was raised in increments, allowing the sample to creep. The presence of gouge in the fault prevented unstable slip at this normal stress. Stable sliding of 100 μm at rates up to 3 × 10^{-2} μm/s produced temperature rises as large as 0.5 m°C. These temperature increases are of the same order as theoretical temperature rises calculated assuming that all work performed during sliding went into heating the gouge. The measured temperature rises are too small, however, to give an accurate estimate of the efficiency of the heating process. Because of the low normal stress and the well-rounded grains of the gouge, we expect little abrasion or grain crushing. *Zoback* [1975] showed that significant amounts of grain crushing do not occur in Ottawa sand until about 55 MPa normal stress. We therefore expect that nearly all frictional sliding energy for this stable mode of deformation will go directly into heating the gouge.

In the second series of experiments, σ_2 was held constant and σ_1 was varied to give constant sliding rate. Sliding rate varied from 0.09 to 9.1 μm/s. In each experiment, the fault underwent an initial period of strain hardening until the coefficient of friction reached approximately 0.55. At this point there was little further increase in strength as the sample continued to slide. At all but the fastest sliding rate, once the fault reached peak strength, it changed to an oscillatory mode, successively jumping ahead and then lagging behind the prescribed displacement. This unstable interaction of the fault with the servo-control system unfortunately masked any sliding rate dependent variations in friction that might have otherwise been observed.

An experiment in which the sample slid at first 0.91 and then 1.82 μm/s is shown in Figure 11; σ_2 was held constant at 2.76 MPa during this experiment. Unstable oscillations develop after 0.1-cm displacement, resulting in a variation of μ between 0.54 and 0.57. Temperatures, corrected for adiabatic changes due to
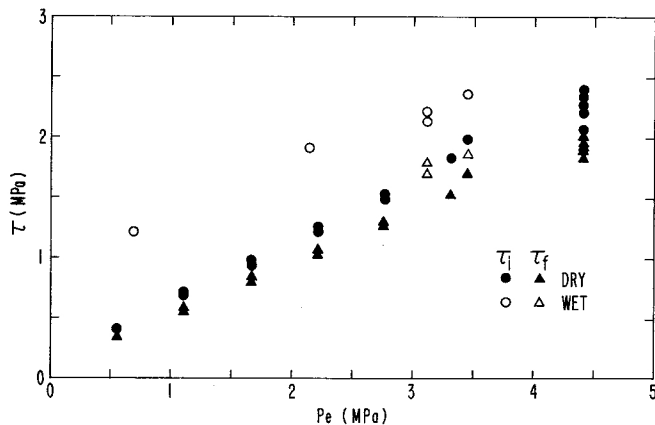

Fig. 10. Initial stress (dots) and frictional strength (triangles) for stick slip as a function of effective pressure $p_e = \sigma_n - P_p$. Open symbols are wet events, solid are dry. Presence of water increases initial stress rather than decreasing frictional stress.
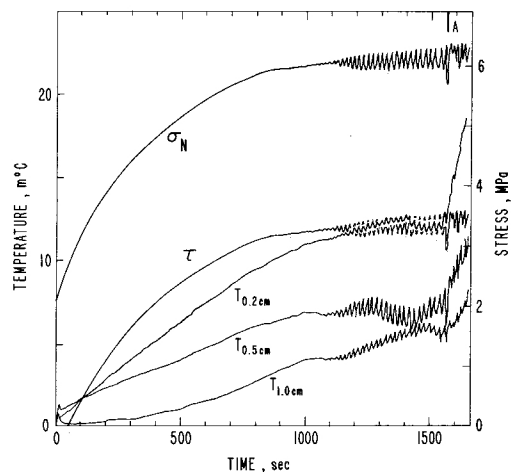

Fig. 11. Stress and temperature plots for constant sliding rate experiment with gouge. Oscillations developed after 1000 s due to interaction of sample and servo-control system. Sliding rate was doubled at 1560 s.
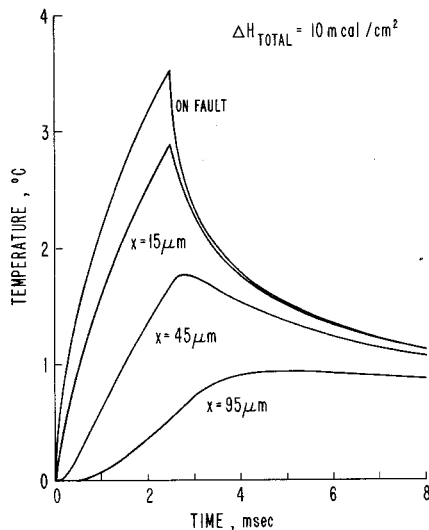
Fig. 12. Simulated temperature plots for 2.5 ms event generating heat at constant rate of 4 mcal/ms cm^2 on fault ($x = 0$).

changing normal stress, are plotted in Figure 11 along with shear and normal stress. The fluctuations in temperature during the oscillating mode are coincident with the changing shear and normal stresses. If they were due to temperature rises transmitted away from the fault zone, they would be out of phase with the stress fluctuations. Because of this, we are unable to account for a significant fraction of the temperature variations, making a precise comparison of total work and frictional heating impossible. The data do indicate, however, that to a first approximation, the temperature rise in the gouge is proportional to normal stress and sliding rate and that at 6 MPa normal stress, a sliding rate of 1 μm/s gives approximately a 10 m°C rise in temperature of the gouge layer.

DISCUSSION

The stick slip events studied here have been conducted at shear stresses as high as 2.5 MPa and total displacements less than 0.03 cm, corresponding to M_L of approximately -1. Although this is well below the total energy released during even moderate earthquakes, some interesting comparisons can be made between earthquakes and these large-scale laboratory experiments. Although energy flux is not as well determined for earthquakes as is total work or moment, it is a more pertinent parameter for describing effects of frictional heating. Lachenbruch [1980] and Sibson [1980] derived a number of relations between energy flux and effects of heating. In our experiments, energy fluxes up to 5 × 10^5 erg/cm^2 were released. The maximum temperature rises 0.5 cm from the fault for these events were only 10 m°C. A numerical model was used to calculate the average heating of the fault surface during sliding for the short time intervals during and after sliding in which the analytic solution does not apply. A representative temperature history is shown in Figure 12. In this example, a constant heat source of 4 mcal/ms cm^2 was supplied at x = 0 for a sliding duration of 2.5 ms. This corresponds roughly to a stick slip event at 5 MPa normal stress. The peak temperature is approximately 4°C, or 400 times the peak temperature at a distance of 0.5 cm from the fault. The model used to generate this heating curve assumes that the heat source is distributed uniformly over the plane x = 0. If the region generating heat has a finite thickness, its temperature will be less than that shown in

Figure 12. These temperatures agree with the analyses of Lachenbruch [1980] and Sibson [1980]. When extended to an earthquake of 5 cm slip at an average stress drop of 10 MPa, the energy flux available for heating would be 1000 times greater. At these energy levels, heating of water and the fault zone material would become important.

Our results do not necessarily contradict those reported by Teufel and Logan [1978]. Surface temperatures measured in their experiments in excess of 1000°C were presumably localized to contact areas and not averaged over the entire surface as in our experiment. Since their experiments were run at approximately 10 times the normal stress used in our experiments, the two data sets would be consistent if the real area of contact were of the order of 1% of the apparent contact area. Teufel and Logan [1978] estimate values in the range of 5-14%.

In our experiments, the presence of water in the fault zone had little effect on frictional heating. The increase in relative stress drop noted in Figure 9 is due primarily to an increase in static frictional strength and not to a decrease in sliding frictional strength. As mentioned earlier, this increase in static friction is probably related to the low stress and smooth fault surface in these experiments and is not expected to apply directly to earthquakes on previously existing faults. Lubrication of the fault by water trapped during slip may also contribute to the increased stress drops. However, neither total stress drops nor significant reduction in sliding friction were observed in these experiments. It is still possible that these effects could occur when trapped water is heated in more energetic events.

Because our experiments were conducted at low stress and small displacements, it is difficult to apply them directly to problems concerning the San Andreas fault or other large fault systems. However, if these results can be extended to midcrustal conditions, they support the assumption that a significant amount of heat should be generated on an active fault. Some mechanism for producing unexpectedly low stress [Lachenbruch and Sass, 1980] or for removing heat (for example, through groundwater convection) must be invoked to account for the lack of a localized heat flow anomaly. A reduction in friction through heating of the fault zone during earthquakes might be a mechanism for a lower frictional heating efficiency, although this would require energy fluxes 1000 times greater than those generated in our experiments. Such a mechanism cannot be used to explain the lack of a localized heat flow anomaly in a region such as Hollister, California, where stable creep is occurring. In this type of region, our results suggest that significant heating is occurring.

The dynamic friction measured in our experiments is large (approximately half of the normal stress in Figure 4), whereas the dynamic stress drop $\tau_i - \tau_f$ is only 10% of the normal stress. If this result is true for earthquakes, it supports the findings of laboratory experiments (using fault surfaces 2 to 3 orders of magnitude smaller than the sample used in this study) as well as in situ stress measurements [McGarr et al., 1982] that ambient tectonic stress may be 10 to 100 times larger than the stress drops inferred from earthquake parameters. In terms of the total energy budget, 92-96% of the total work goes into heating the fault. A negligible amount of work is used in creating new surface area, and consequently, the seismic efficiency is 4-8%. If these events occurred on a natural fault, more work might be expected to go into creating new surface area. Thus seismic efficiency would at most be 5-10%. Estimates of stress drop based on seismic parameters, then, may only represent 10% or less of the total energy released during earthquakes.

In summary, we have shown the following: (1) Laboratory

stick slip and stable sliding modes of deformation produce measurable heating of the fault surface. (2) This heating can be related to the frictional sliding energy expended during deformation. (3) For the range of normal stresses studied, average surface temperature rises were less than 4°C and, consequently, had little effect in controlling friction. (4) The presence of water and gouge had little effect on the rate of frictional heating.

REFERENCES

Andrews, D. J., Rupture velocity of plane strain shear cracks, *J. Geophys. Res., 81*, 5679–5687, 1976.

Bowden, F. P., and D. Tabor, *The Friction and Lubrication of Solids*, Clarendon Press, Oxford, 1958.

Brune, J. N., T. L. Henyey, and R. F. Roy, Heat flow, stress and rate of slip along the San Andreas fault, California, *J. Geophys. Res., 74*, 3821–3827, 1969.

Byerlee, J. D., Theory of friction based on brittle fracture, *J. Appl. Phys., 38*, 2928–2934, 1967.

Byerlee, J. D., Comments on T. Engelder's paper "Aspects of asperity-surface interactions," in *Proceedings of Conference II Experimental Studies of Rock Friction With Application to Earthquake Prediction*, pp. 138–142, U.S. Geological Survey, Menlo Park, Calif., 1977.

Carslaw, H. S., and J. C. Jaeger, *Conduction of Heat in Solids*, 386 pp., Oxford University Press, New York, 1959.

Dieterich, J. H., Potential for geophysical experiments in large scale tests, *Geophys. Res. Lett., 8*, 653–656, 1981.

Engelder, T., Aspects of asperity-surface interaction and surface damage of rocks during experimental frictional sliding, *Pure Appl. Geophys., 116*, 705–716, 1978.

Ida, Y., Cohesive force across the tip of a longitudinal shear crack and Griffith's specific surface energy, *J. Geophys. Res., 77*, 3796–3805, 1972.

Jaeger, J. C., Moving sources of heat and the temperature of sliding contacts, *Proc. R. Soc. N.S.W., 76*, 203–244, 1942.

Lachenbruch, A. H., Preliminary geothermal model of the Sierra Nevada, *J. Geophys. Res., 73*, 6977–6989, 1968.

Lachenbruch, A. H., Frictional heating, fluid pressure, and the resistance to fault motion, *J. Geophys. Res., 85*, 6079–6112, 1980.

Lachenbruch, A. H., and J.H. Sass, Heat flow and energetics of the San Andreas fault zone, *J. Geophys. Res., 85*, 6185–6222, 1980.

Lockner, D. A., P. G. Okubo, and J. H. Dieterich, Containment of stick slip failures on a simulated fault by pore fluid injection, *Geophys. Res. Lett., 9*, 801–804, 1982.

McGarr, A., M. D. Zoback and T. C. Hanks, Implications of an elastic analysis of in situ stress measurements near the San Andreas fault, *J. Geophys. Res., 87*, 7797–7806, 1982.

McKenzie, D. P., and J. N. Brune, Melting of fault planes during large earthquakes, *Geophys. J. R. Astron. Soc., 29*, 65–78, 1972.

Okubo, P. G., and J. H. Dieterich, Fracture energy of stick-slip events in a large-scale biaxial experiment, *Geophys. Res. Lett., 8*, 887–890, 1981.

Raleigh, C. B., Frictional heating, dehydration and earthquake stress drops, in *Proceedings of Conference II Experiment Studies of Rock Friction With Application to Earthquake Preciction*, U.S. Geological Survey, Menlo Park, Calif., 1977.

Richards, P. G., Dynamic motions near an earthquake fault: A three dimensional solution, *Bull. Seismol. Soc. Am., 66*, 1–32, 1976.

Sibson, R. H., Interactions between temperature and pore fluid pressure during earthquake faulting and a mechanism for partial or total stress relief, *Nature, 243*, 66–68, 1973.

Sibson, R. H., Power dissipation and stress levels on faults in the upper crust, *J. Geophys. Res., 85*, 6239–6247, 1980.

Sibson, R. H., S. H. White and B. K. Atkinson, Fault rock distribution and structure within the Alpine fault zone: a preliminary account, The origin of the southern Alps, edited by R. I. Walcott and M. M. Cresswell, *Bull. R. Soc. N. Z., 18*, 55–65, 1979.

Teufel, L. W., and J. M. Logan, Effect of displacement rate on the real area of contact and temperatures generated during frictional sliding of Tennessee sandstone, *Pure Appl. Geophys., 116*, 840–865, 1978.

Zoback, M. D., High pressure deformation and fluid flow in sandstone, granite and granular material, Ph.D. thesis, 210 pp., Stanford Univ., Stanford, Calif., 1975.